

Supporting Information

An unexpected transmetalation intermediate: isolation and structural characterization of a solely CH₃ bridged di-copper(I) complex

Roberto Molteni^a, Rüdiger Bertermann^a, Katharina Edkins^b and Andreas Steffen^{a*}

^a *Institut für Anorganische Chemie, Julius-Maximilians-Universität Würzburg, Am Hubland, 97074 Würzburg, Germany. E-Mail: andreas.steffen@uni-wuerzburg.de*

^b *School of Medicine, Pharmacy and Health, Durham University Queen's Campus, University Boulevard, Stockton-on-Tees, TS17 6BH, United Kingdom.*

Contents:

General Considerations	2
Experimental Details	3
Reaction of 2 with 3-Methyl-2-cyclohexenone	4
Single crystal X-ray diffraction	5
Powder X-ray diffraction	6
Computational studies	7
NMR Spectra of 1 in D ₆ -benzene	12
NMR Spectra of 2 in the solid state	13
NMR Spectra of 2 in D ₈ -toluene at -40 °C.....	16
NMR Spectra of 2 in d ₈ -THF at -40 °C	19

General Considerations

The syntheses were carried out under an argon atmosphere with standard Schlenk techniques, or in a nitrogen-filled Innovative Tech. Inc. glovebox. Crystallization experiments were set up in the same glovebox equipped with a freezer. All experiments were carried out on crystalline samples, of which the respective unit cell was determined for several crystals of the bulk sample before the measurements in order to exclude impurities. Furthermore, multiple trials of the same experiment/data collection ensured reproducibility.

NMR spectra in solution were recorded at 298 K (compound **1**) or 233 K (compound **2**) on a Bruker Avance I 500 NMR spectrometer with a BB Prodigy Cryo probe (^1H : 500.1 MHz, ^{13}C : 125.8 MHz, ^{31}P : 202.5 MHz using C_6D_6 , $\text{C}_6\text{D}_5\text{CD}_3$ or $[\text{D}_8]\text{THF}$, as the solvent.). Chemical shifts (ppm) were determined relative to internal C_6HD_5 (^1H , δ 7.16; C_6D_6), internal C_6D_6 (^{13}C , δ 128.0; C_6D_6), internal $\text{C}_6\text{D}_5\text{CHD}_2$ (^1H , δ 2.09; $\text{C}_6\text{D}_5\text{CD}_3$), internal $\text{C}_6\text{D}_5\text{CD}_3$ (^{13}C , δ 20.4; $\text{C}_6\text{D}_5\text{CD}_3$), internal $[\text{D}_7]\text{THF}$ (^1H , δ 1.73; $[\text{D}_8]\text{THF}$), internal $[\text{D}_8]\text{THF}$ (^{13}C , δ 25.3; $[\text{D}_8]\text{THF}$), external 85% phosphoric acid (H_3PO_4) (^{31}P , δ 0; C_6D_6 , $\text{C}_6\text{D}_5\text{CD}_3$, $[\text{D}_8]\text{THF}$).

Assignment of the ^{13}C NMR data was supported by ^{13}C DEPT135 and ^1H , ^{13}C HSQC correlation experiments. The thermocouple used with the probe for the low-temperature NMR studies was calibrated according to ref. 1 using an 4% MeOH in $[\text{D}_4]\text{MeOH}$ containing a trace of HCl.

The depicted $^{13}\text{C}\{^1\text{H}\}$ CP/MAS NMR spectrum was recorded at 295 K on a Bruker DSX 400 NMR spectrometer (^{13}C : 100.6 MHz) with bottom-layer rotors of ZrO_2 (diameter, 2.5 mm) containing ca. 20 mg of sample with a spinning rate of 10.4 kHz, a contact time of 2 ms, 90° ^1H transmitter pulse length of 2.5 μs and a repetition time of 20 s. The shown ^1H BR24 Cramps and $^{31}\text{P}\{^1\text{H}\}$ CP/MAS NMR spectra were recorded at 295 K on a Bruker DSX 400 NMR spectrometer (^1H : 400.2, ^{31}P : 162.0 MHz) with a bottom-layer rotor of ZrO_2 (diameter, 4 mm) containing ca. 50 mg of sample with a spinning rate of 2 kHz (^1H Cramps) or 13 kHz ($^{31}\text{P}\{^1\text{H}\}$ CP/MAS), respectively. For the $^{31}\text{P}\{^1\text{H}\}$ CP/MAS NMR a contact time of 3 ms, 90° ^1H transmitter pulse length of 3 μs and a repetition time of 10 s was used. The ^1H BR24 Cramps solid-state NMR was performed with 4 scans and a recycle delay of 5 s.

All NMR shifts were referenced with an external standard by adjusting the magnetic field B_0 of the magnet, so that the ^{13}C low-field signal of adamantane appears at 38.48 ppm.

The $^{31}\text{P}\{^1\text{H}\}$ CP/MAS solid-state NMR spectrum of compound **2** was fitted using the software WINDAISEY 4.05 from Bruker-Franzen Analytik GmbH.

IR spectra were measured in the attenuated total reflection (ATR) mode in the region of 4000-400 cm^{-1} , with an apodized resolution of 1 cm^{-1} , with a Bruker Alpha spectrometer equipped with a Bruker diamond single reflection ATR system. These experiments were conducted in a nitrogen-filled glovebox (see picture below) on single crystals from a crystalline bulk material, of which multiple unit cell determinations ensured the identity of the measured crystal.

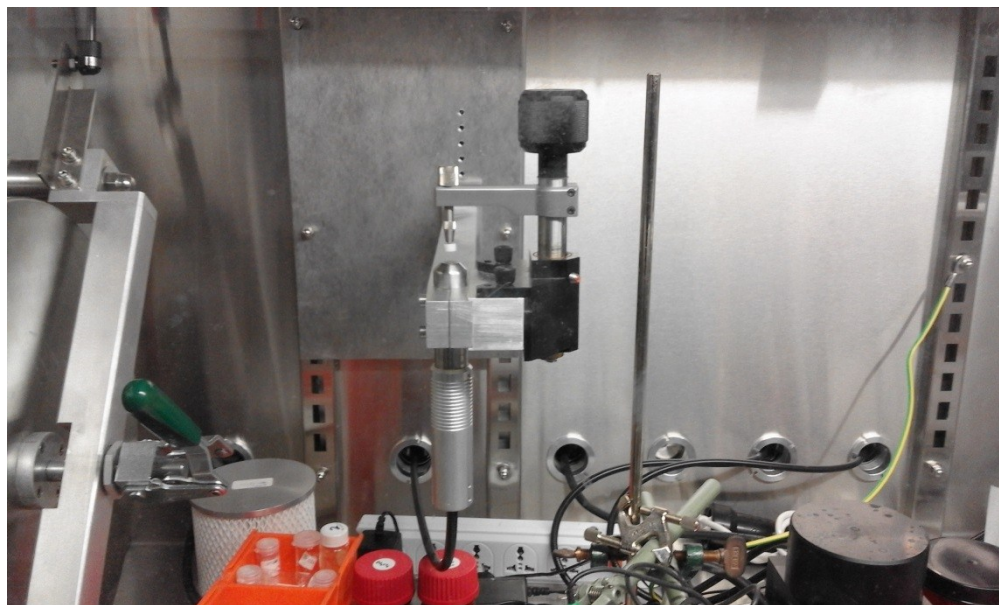


Figure S1. Bruker diamond single reflection ATR system in a nitrogen-filled glovebox used for collected IR spectra of **2**.

Experimental Details

[CuMe(PPh₃)₃] (1): The synthesis of **1** was carried out as described in the literature (see manuscript). Specifically, Cu(acac)₂ (1.57 g, 6 mmol) and PPh₃ (4.6 g, 18 mmol) were suspended in diethylether (50 ml) and then stirred for 30 minutes at -40°C. A solution of AlMe₂OEt (60 mmol, generated in situ by adding 3.54 ml of EtOH to a solution of 30 ml of AlMe₃ (2 M) in toluene) was added dropwise to the suspension over 30 minutes and was then stirred for 1 hour at -40°C. The reaction mixture was allowed to warm up to room temperature, when the colour changed from blue to yellow. A yellow precipitate formed which was filtered off, washed with 50 ml diethylether and then dried in vacuum to give 6.3 g of impure **1**.

[Cu(PPh₃)₂(μ-Me)CuMe] (2): 300 mg of **1** were weighed in a 30 ml scintillation vial and dissolved in the minimum amount of solvent A. Solvent B was layered on top, and then the vial was stored at -30 °C. After 2 days single-crystals suitable for X-ray diffraction studies had formed. Various crystallization results in dependence of the solvents A and B are given in Table S1.

Table S1. Results of crystallization experiments.

Solvent A	Solvent B	Outcome
THF	Et ₂ O	[Cu(PPh ₃) ₂ (μ-Me)CuMe]
THF	Hexane	[CuMe(PPh ₃) ₃] ^a
THF	C ₆ F ₆	[CuMe(PPh ₃) ₃] ^a

^a Determined by comparison of the elemental cell with literature data.

Reaction of **2** with 3-Methyl-2-cyclohexenone

In a Young tab NMR tube, **2** (28 mg, 0.046 mmol) was dissolved in D₈-THF (0.7 ml) and cooled to -78°C. 3-Methyl-2-cyclohexenone (5 mg, 6 μl, 0.046 mmol) was added and the reaction was allowed to warm up to room temperature over 8 hours.

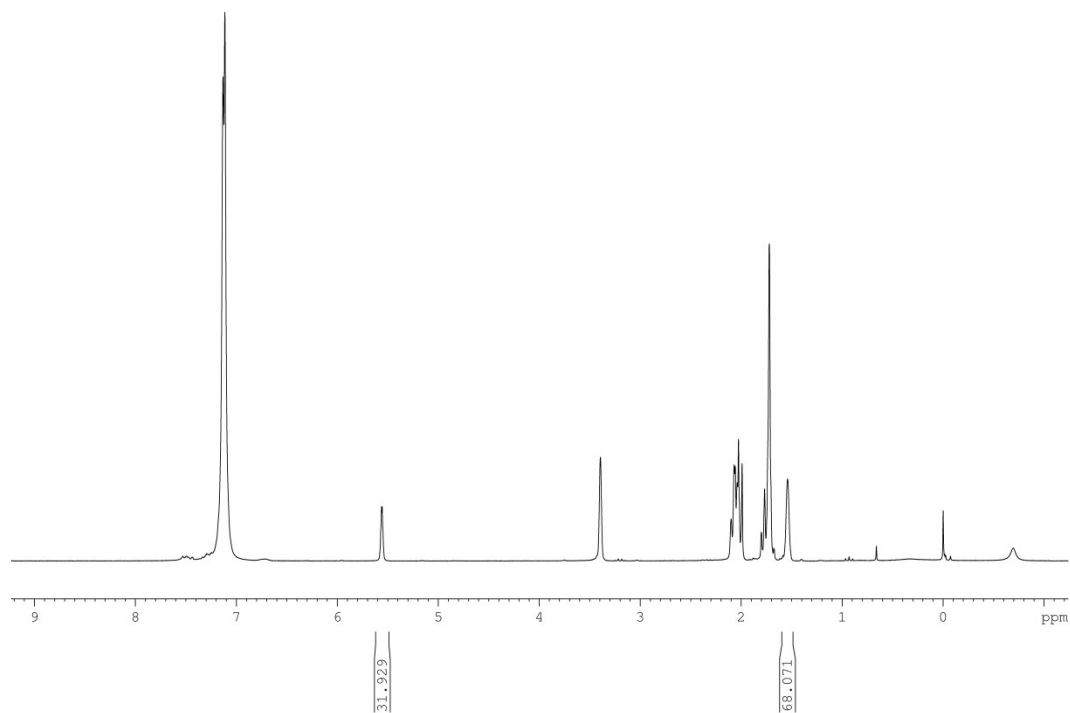


Figure S2. In situ ¹H NMR spectrum of the reaction of **2** with 3-methyl-2-cyclohexenone, showing the methyl groups of the starting material at 5.59 ppm while the two methyl functionalities of the methylation product, 3-dimethylcyclohexanone, are found at 1.55 ppm.

Single crystal X-ray diffraction

Crystals suitable for single-crystal X-ray diffraction were selected, coated in degassed perfluoropolyether oil, and mounted on MiTeGen sample holders. Diffraction data were collected on a Nonius Kappa three circle diffractometer utilizing graphite monochromated MoK α radiation ($\lambda = 0.71073 \text{ \AA}$) from a rotating anode tube run at 50 V and 30 mA. The diffractometer is equipped with a Bruker ApexII area detector and an open flow N2 Cryoflex II (Bruker) device, the measurement was performed at 100 K. For data reduction, the Bruker Apex2 software suite (Bruker AXS) was used. Subsequently, utilizing Olex2,² the structures were solved using the Olex2.solve charge-flipping algorithm, and were subsequently refined with Olex2.refine using Gauss-Newton minimization. All non-hydrogen atom positions were located from the Fourier maps and refined anisotropically. Hydrogen atom positions were calculated using a riding model in geometric positions and refined isotropically, where possible to determine unambiguously.

Crystal Data for C₃₈H₃₃Cu₂P₂ (M = 676.34 g/mol): triclinic, space group P-1, $a = 10.0317(3) \text{ \AA}$, $b = 12.1017(4) \text{ \AA}$, $c = 13.3609(4) \text{ \AA}$, $\alpha = 97.647(1)^\circ$, $\beta = 94.311(1)^\circ$, $\gamma = 95.342(1)^\circ$, $V = 1594.30(9) \text{ \AA}^3$, $Z = 2$, $T = 100 \text{ K}$, $\mu(\text{Mo K}\alpha) = 1.435 \text{ mm}^{-1}$, $D_{\text{calc}} = 1.4088 \text{ g/cm}^3$, 24518 reflections measured ($3.08^\circ \leq 2\theta \leq 52^\circ$), 6267 unique ($R_{\text{int}} = 0.0203$, $R_{\text{sigma}} = 0.0232$) which were used in all calculations. The final R_1 was 0.0255 ($I \geq 2\sigma(I)$) and wR_2 was 0.0929 (all data).

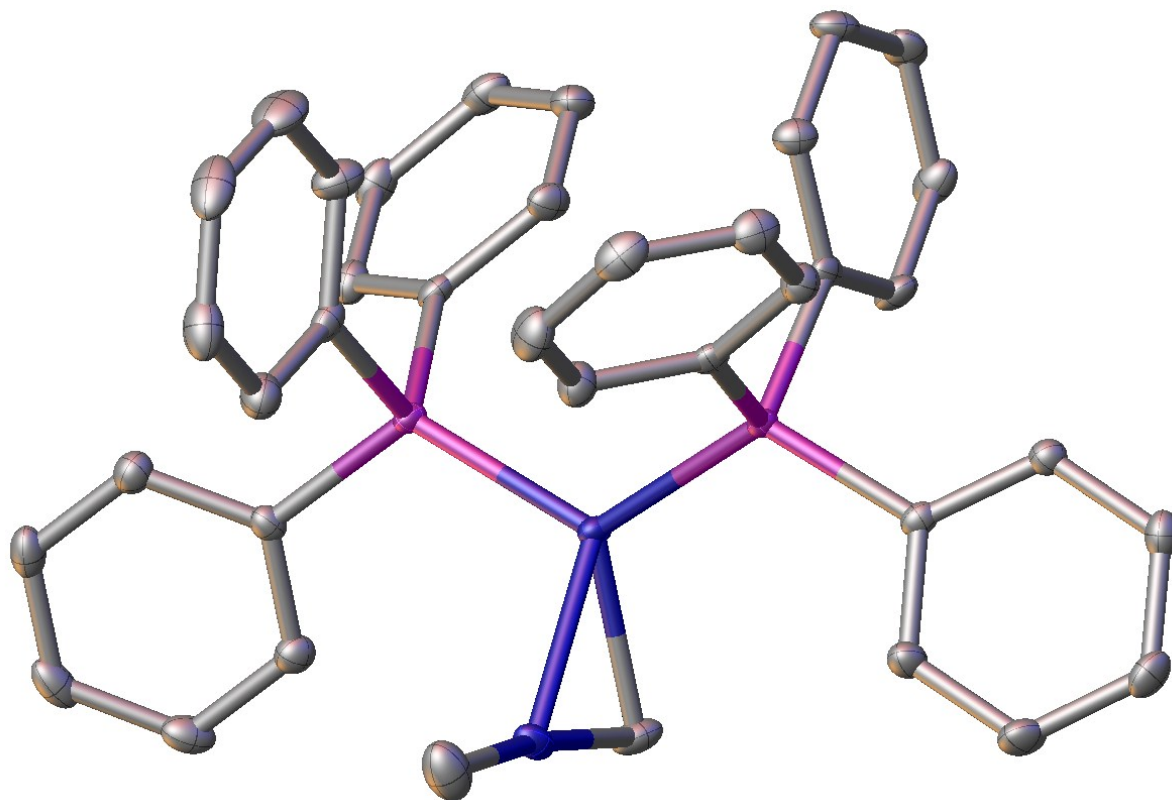


Figure S3. Molecular structure of **2**. Atomic displacement parameters are drawn at 50% probability, hydrogen atoms are omitted for clarity. Colour scheme: carbon (grey), phosphorus (purple), copper (blue).

Powder X-ray diffraction

The powder diffraction samples were grinded and put into Lindemann glass capillaries (\varnothing 0.3 mm). X-ray powder diffractometric investigations were done using a Bruker D8 Discover (DA VINCI® design) powder diffractometer (Bruker AXS GmbH, Karlsruhe, Germany) with a copper tube operated at 40 kV and 40 mA (unsplit $K\alpha_1+K\alpha_2$ doublet, mean wavelength $\lambda = 154.19$ pm). A focusing Goebel mirror and a 0.6 mm fixed divergence slit were mounted in the primary beam path, the receiving slit in the secondary beam path was used with 7.5 mm opening. 2.5° axial Soller slits were used in both beam paths. Detection was done with a LynxEye® (Bruker AXS) 1D-detector using the full detector range of 192 channels.

Measurements were done in 'Coupled Two Theta/Theta' mode, with a 2θ range of $5 - 60^\circ$, a step width of 0.025° and 0.25 seconds measurement time per step.

Data collection and processing was done with the software packages DIFFRAC.Suite (V2 2.2.690, Bruker AXS 2009-2011) and DIFFRAC.EVA (Version 3.0, Bruker AXS 2010-2013).

(Coupled TwoTheta/Theta)

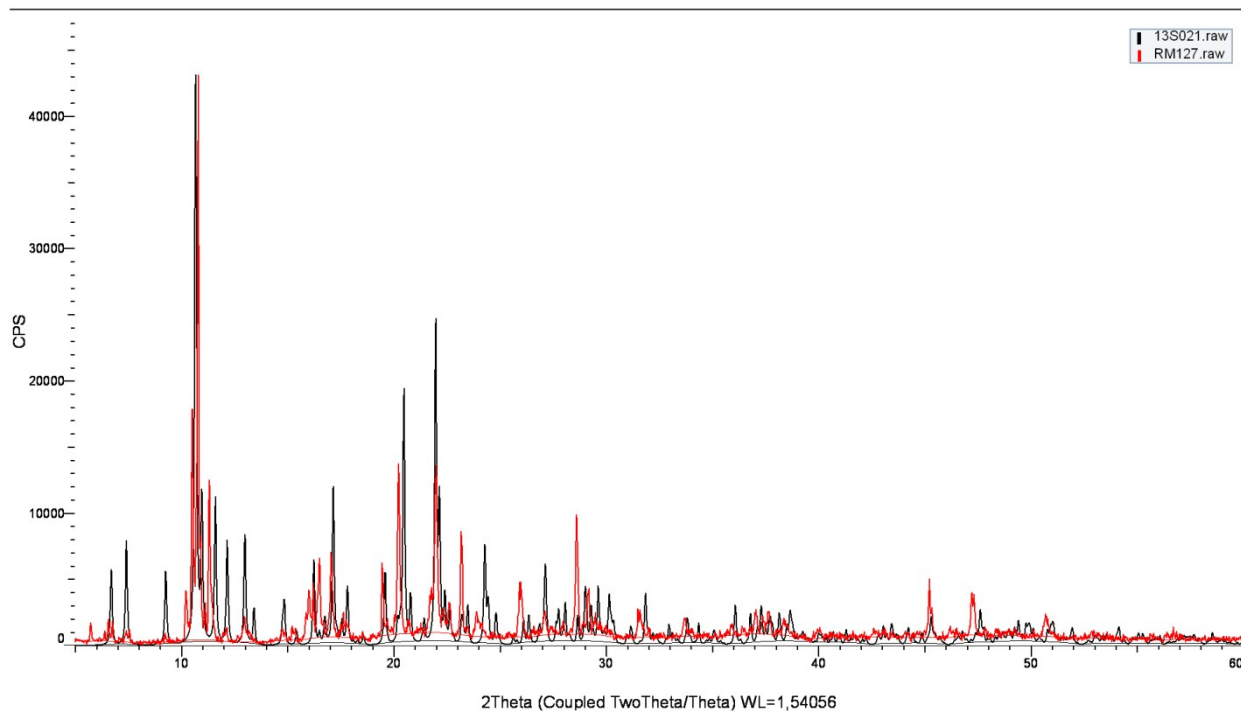


Figure S4. Experimental powder diffraction pattern (red) and predicted powder diffraction pattern calculated on the basis of the crystal structure of **2** (black).

Computational studies

Calculations (gas-phase) were performed with the ORCA 3.0.2 program suite.³ Geometry optimisations for compounds $[\text{Cu}^{\text{I}}(\text{PPh}_3)_2(\mu\text{-CH}_3)\text{Cu}^{\text{II}}\text{Me}]$ (**2**) and $[\text{Cu}^{\text{I}}(\text{PPh}_3)_2(\mu\text{-CH}_2)\text{Cu}^{\text{II}}\text{Me}]$ were carried out with the BP86^{4, 5} functional as implemented in ORCA. The def2-TZVP^{6, 7} basis set was used for all atoms together with the auxiliary basis set def2-TZVP/J in order to accelerate the computations within the framework of RI approximation. Relativistic effects were accounted for by employing the ZORA⁸ method and van der Waals interactions have been considered by an empirical dispersion correction (Grimme-D3BJ).^{9, 10} Numerical frequency analyses, NBO analyses and Mayer bond orders were performed with the same functional and basis sets. Representations of molecular orbitals were produced with orca_plot as provided by ORCA 3.0.2 and with gOpenMol 3.00.^{11, 12}

Table S2. Cartesian coordinates of the optimized geometry of $[\text{Cu}^{\text{I}}(\text{PPh}_3)_2(\mu\text{-CH}_2)\text{Cu}^{\text{II}}\text{Me}]$.

Cu	-0.80713824418494	0.87532885355763	0.14325516026465
P	0.11382431284031	2.03732223948703	-1.50047333745945
C	-0.45519607699082	1.18364298213388	-3.00780363637896
C	-1.69436868106601	1.49109059254015	-3.59184304051611
C	0.25047671729077	0.05002439512256	-3.44423396134396
C	-2.21559959003218	0.67899600524306	-4.59867998107605
H	-2.26392133116885	2.35257312021207	-3.24706282769901
C	-0.28036935833108	-0.76228767303033	-4.44702228503562
H	1.20046985067958	-0.21131191165164	-2.97983952418283
C	-1.51373004032042	-0.45173812836726	-5.02530221229347
H	-3.18189841888506	0.92744005760682	-5.03857745830122
H	0.27142213070556	-1.64714231730270	-4.76569552906006
H	-1.93015473977270	-1.09246073774522	-5.80361777480193
C	1.93778145187217	1.99956151130186	-1.64300904341988
C	2.66323190494751	1.22273100591083	-0.73113052836382
C	2.61548398983629	2.69915796121353	-2.65246454643919
C	4.05310255609970	1.13214848190954	-0.83709693330388
H	2.12575946703919	0.67074084311547	0.04397809977369
C	4.00315497354944	2.61278739248254	-2.75202747947365
H	2.05717616326338	3.31289570946106	-3.36058342125958
C	4.72334397182376	1.82656199838280	-1.84542566688199
H	4.60907802324691	0.51512593771818	-0.13033361248263
H	4.52608182772057	3.15771545505401	-3.53926013302019
H	5.80890030295015	1.75686702084586	-1.92822818632213
C	-0.29965210686139	3.80043366043204	-1.73604794306259
C	-0.44668571961157	4.57502113494332	-0.57495127961771
C	-0.47846853068650	4.40461902820188	-2.98823635095827
C	-0.76711551812816	5.92942016652499	-0.66259371983800
H	-0.32199814093415	4.10032683074517	0.40121439651332
C	-0.81185226638638	5.75721853158467	-3.07506958898613
H	-0.37658117900185	3.81159436714101	-3.89731632629891
C	-0.95731487624331	6.52170632731762	-1.91464296644569
H	-0.87953183993400	6.52117317434544	0.24679627593580
H	-0.96048112918028	6.21553914970787	-4.05380829469409
H	-1.22006991442711	7.57803243375777	-1.98527083503752
P	-3.03545720228780	0.92407116590891	0.04354858826756
C	-3.89414211827115	2.02196266860736	-1.13475318513709
C	-4.71276585353359	1.54500127905588	-2.16791569126755
C	-3.62392746226686	3.39808777165492	-1.05175920674639
C	-5.23277325848466	2.43090691227052	-3.11465248929340
H	-4.92076561624662	0.47771469541022	-2.24274284926050

C	-4.14255847931917	4.27954924266494	-1.99706564218527
H	-2.97983929745611	3.77480223549463	-0.25698366642343
C	-4.94188082831681	3.79529177442174	-3.03903056518042
H	-5.86391782104095	2.05071974061438	-3.91944814206982
H	-3.90452397890781	5.34148992067522	-1.93113000407020
H	-5.33653534499494	4.48142816203977	-3.78938998745889
C	-3.93794585015979	1.20501834821312	1.60472041682454
C	-3.28178156142244	0.91436938813224	2.81023543291350
C	-5.25657093372328	1.68378438000905	1.63132084092507
C	-3.94390514313440	1.08583610148373	4.02634536299778
H	-2.24860075575063	0.55951626477559	2.77843193155596
C	-5.91268535303336	1.86006836959896	2.85064102253234
H	-5.76470697501786	1.92239990334064	0.69612670561622
C	-5.25914470488916	1.55851161228383	4.04888989445429
H	-3.42825452139191	0.85660813713890	4.95994422993903
H	-6.93746924094424	2.23408599956132	2.86531402285386
H	-5.77332276606825	1.69815337159314	5.00083806798058
C	-3.51377839836919	-0.75272402077337	-0.49424496654340
C	-2.73463869741103	-1.35109792565892	-1.49874702639047
C	-4.58432829052864	-1.46088101970289	0.06601899557521
C	-3.03655653931096	-2.63475974396155	-1.94828012578305
H	-1.88347598789822	-0.81634643198004	-1.92216283718070
C	-4.87689798236041	-2.75201235210833	-0.38058675905808
H	-5.18198823610969	-1.00707848267030	0.85737739134002
C	-4.10674321133958	-3.33843576157972	-1.38839210568012
H	-2.41810987021872	-3.08923292438200	-2.72253723555597
H	-5.70643148819798	-3.30283166990579	0.06513237422084
H	-4.33381558788664	-4.34949972666222	-1.72930938927839
Cu	0.39036533433548	-1.22459160363640	-0.21649902603277
C	1.19766980102851	-2.55405103827436	-1.35111761845734
H	2.13830196391677	-2.18997007693389	-1.79690585174224
H	1.42363107182909	-3.46831854401625	-0.78005641176112
H	0.50443821626496	-2.82454232235170	-2.16516044489765
C	-0.23163235929018	-0.46970664840887	1.42822179969482
H	0.53625065458408	-0.14305220503346	2.14827490766535
H	-0.96426768609440	-1.12680204681248	1.92072173366435

Table S3. Cartesian coordinates of the optimized geometry of $[\text{Cu}^{\text{I}}(\text{PPh}_3)_2(\mu\text{-CH}_3)\text{Cu}^{\text{I}}\text{Me}]$ (**2**).

Cu	-0.040920	-1.124516	-0.534861
P	-1.833354	0.114663	-0.259762
C	-2.433530	0.123501	1.460802
C	-1.516941	-0.150616	2.483771
C	-3.768711	0.415021	1.780035
C	-1.926403	-0.115491	3.816484
H	-0.492420	-0.422773	2.234300
C	-4.174949	0.446313	3.114335
H	-4.489233	0.604994	0.982962
C	-3.252663	0.185420	4.133568
H	-1.206034	-0.342057	4.602365
H	-5.214635	0.668048	3.359545
H	-3.574839	0.202674	5.175826
C	-3.299616	-0.398067	-1.216727
C	-3.660881	-1.754141	-1.145009
C	-4.052504	0.478341	-2.008412
C	-4.771877	-2.219409	-1.845077
H	-3.062454	-2.435243	-0.536462
C	-5.158583	0.003845	-2.718954
H	-3.773797	1.531108	-2.067033
C	-5.521464	-1.341952	-2.636718
H	-5.050001	-3.272201	-1.780712
H	-5.740420	0.690903	-3.335243

H	-6.386153	-1.709620	-3.190723
C	-1.617995	1.882966	-0.670045
C	-0.901982	2.186293	-1.839197
C	-2.013918	2.924496	0.179599
C	-0.571334	3.504042	-2.147688
H	-0.570707	1.376285	-2.490067
C	-1.677771	4.245336	-0.127625
H	-2.555523	2.697217	1.097772
C	-0.950541	4.537252	-1.284459
H	0.008100	3.718733	-3.045928
H	-1.976620	5.049129	0.546942
H	-0.674025	5.567695	-1.511080
P	1.885434	-0.099116	-0.271152
C	1.751238	0.793636	1.316093
C	2.164568	0.182091	2.508705
C	1.042869	2.005705	1.375914
C	1.869678	0.772655	3.739057
H	2.702266	-0.765203	2.476162
C	0.756820	2.593111	2.606367
H	0.699833	2.483115	0.459422
C	1.165067	1.977181	3.792511
H	2.188175	0.281546	4.659364
H	0.197937	3.529182	2.634923
H	0.927269	2.430834	4.755254
C	2.353796	1.164227	-1.503861
C	2.085139	0.867905	-2.849287
C	2.950510	2.390098	-1.179555
C	2.404048	1.781185	-3.853356
H	1.613087	-0.084634	-3.101210
C	3.255496	3.310851	-2.183938
H	3.167008	2.628457	-0.138122
C	2.983078	3.009833	-3.520680
H	2.191381	1.539287	-4.895513
H	3.710096	4.266853	-1.920439
H	3.221162	3.731524	-4.303191
C	3.400883	-1.108749	-0.092279
C	3.278502	-2.395055	0.454620
C	4.666269	-0.636149	-0.470140
C	4.410578	-3.189076	0.640090
H	2.285847	-2.766603	0.739316
C	5.793914	-1.439831	-0.296474
H	4.769518	0.357472	-0.907270
C	5.669442	-2.715168	0.262251
H	4.303447	-4.184560	1.073076
H	6.774192	-1.067621	-0.597943
H	6.553260	-3.340248	0.397754
Cu	-0.071513	-3.041582	0.813700
C	0.081131	-3.188972	2.709861
H	0.552676	-4.142261	3.009104
H	0.694297	-2.376110	3.137187
H	-0.908481	-3.139798	3.195096
C	-0.178835	-3.116272	-1.201750
H	-0.213071	-2.428442	-2.086310
H	0.692878	-3.762301	-1.397315
H	-1.096215	-3.718060	-1.311246

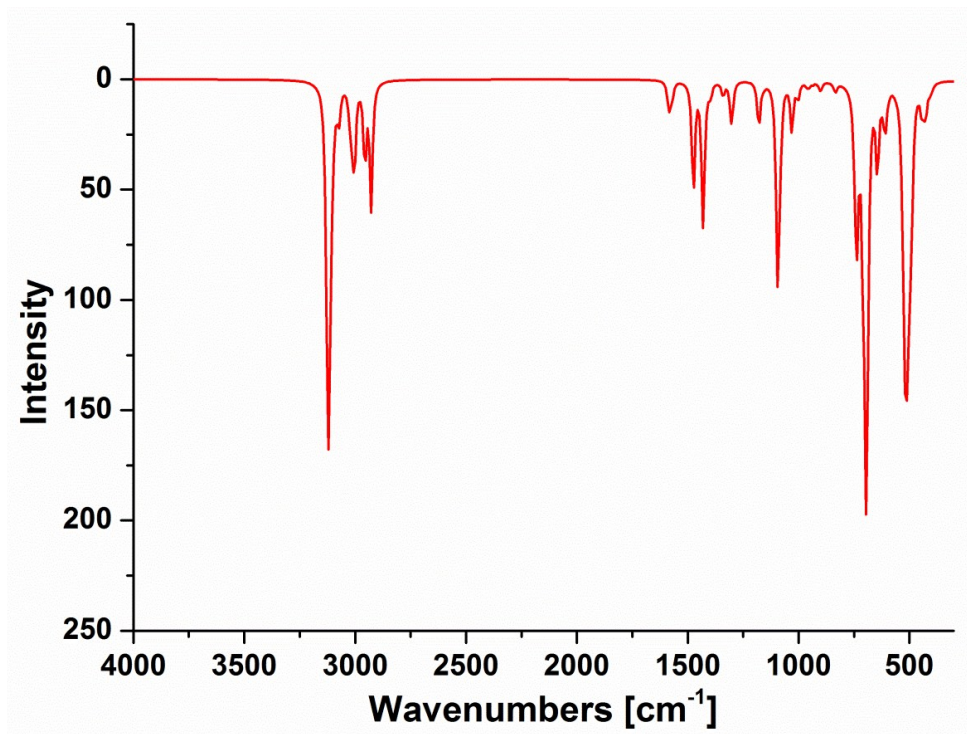


Figure S5. Calculated IR spectrum of $[\text{Cu}^{\text{I}}(\text{PPh}_3)_2(\mu\text{-CH}_2)\text{Cu}^{\text{II}}\text{Me}]$ (without scaling factor).

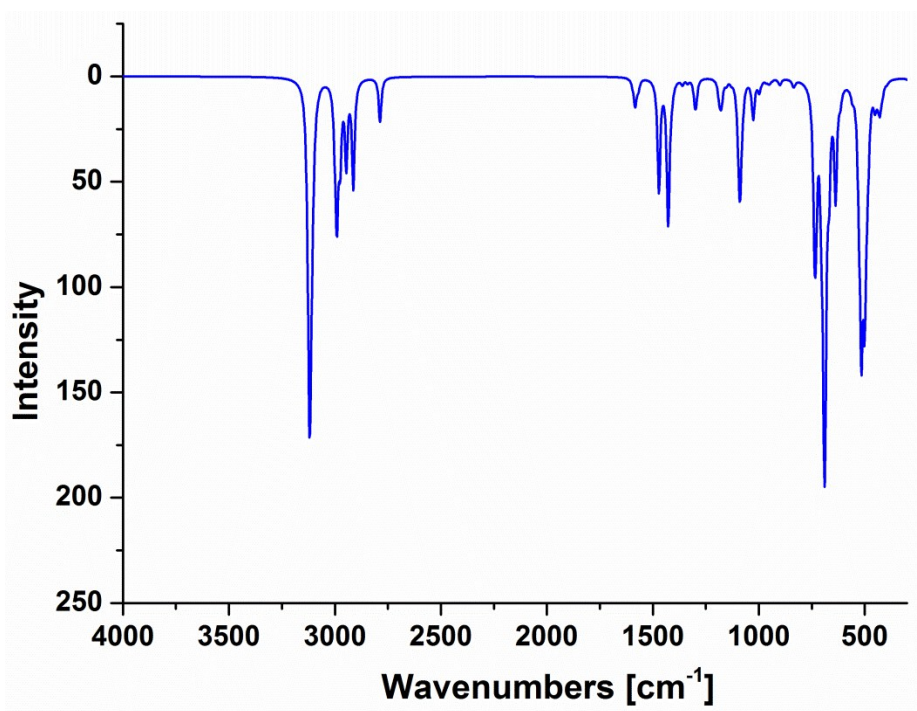


Figure S6. Calculated IR spectrum of $[\text{Cu}^{\text{I}}(\text{PPh}_3)_2(\mu\text{-CH}_3)\text{Cu}^{\text{I}}\text{Me}]$ (**2**) (without scaling factor).

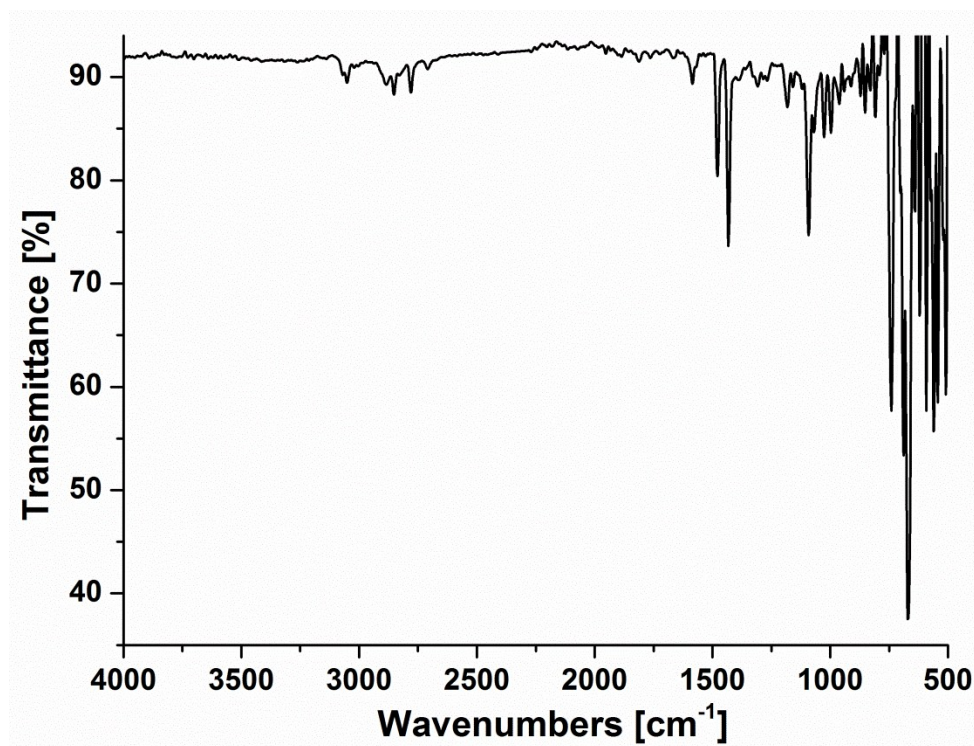


Figure S7. Experimental ATR-FT-IR spectrum of $[\text{Cu}^{\text{I}}(\text{PPh}_3)_2(\mu\text{-CH}_3)\text{Cu}^{\text{I}}\text{Me}]$ (**2**).

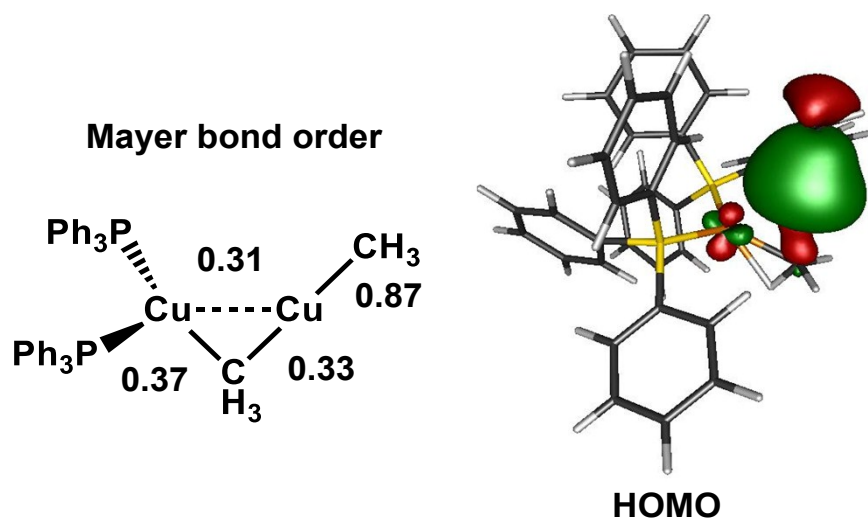


Figure S8. Mayer bond order and HOMO of **2**. According to our NBO analysis, the energetic major contribution of 76.5 kcal/mol for the formation of the Cu-(m-Me)-Cu motif stems from the donation $\text{C1}(\text{sp}^3) \rightarrow \text{Cu2}(\text{s})/\text{C2}(\text{sp}^3)$, while the $\text{Cu2}(\text{d}) \rightarrow \text{Cu1}(\text{s})$ interaction provides an additional 10 kcal/mol. These values are in agreement with our interpretation of the structural parameters obtained from the X-ray diffraction experiments, suggesting a dimethylcuprate weakly associated to a $\{\text{Cu}(\text{PPh}_3)_2\}^+$ cation.

NMR Spectra of 1 in D₆-benzene

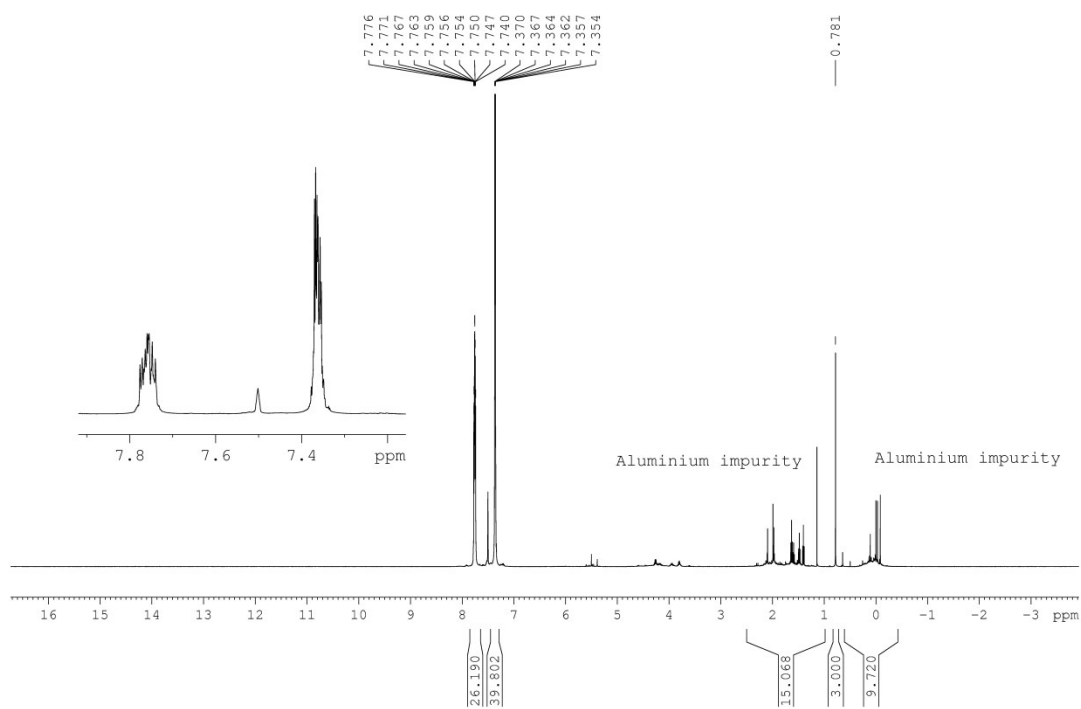


Figure S9. ¹H NMR of 1 in D₆-benzene, 500.1 MHz.

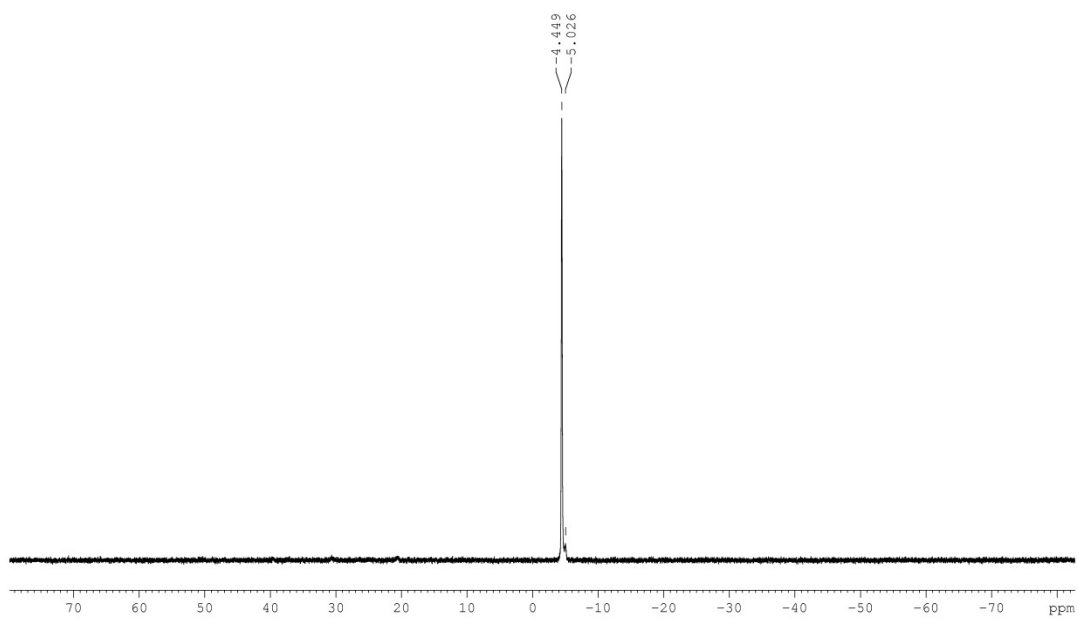


Figure S10. ³¹P{¹H} NMR of 1 in D₆-benzene, 202.5 MHz.

NMR Spectra of 2 in the solid state

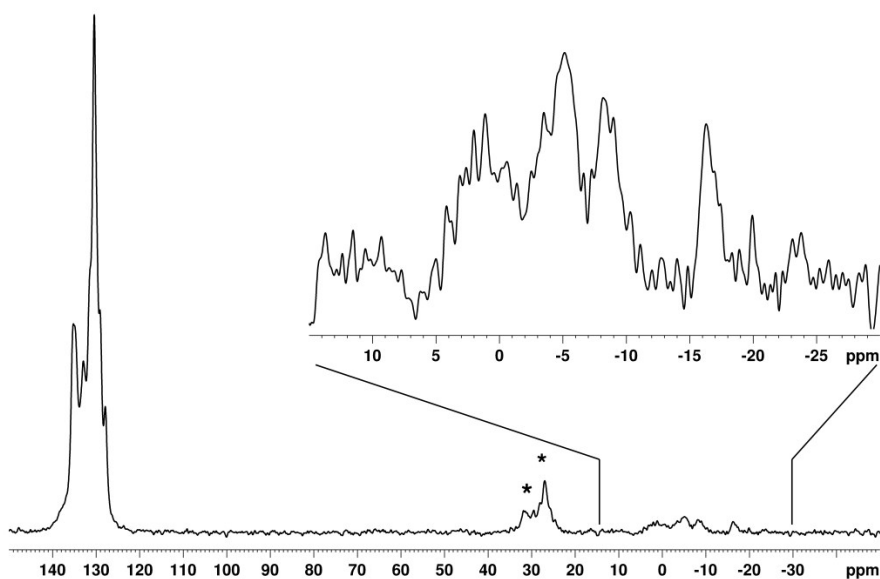


Figure S11. $^{13}\text{C}\{^1\text{H}\}$ CP/MAS solid-state NMR of **2** measured with 3100 scans at 100.6 MHz with a MAS spinning speed of 10.4 kHz. Spinning side bands (SSB) are marked with an asterisk. The excerpt shows the broad ^{13}C signals arising from the CuMe moieties.

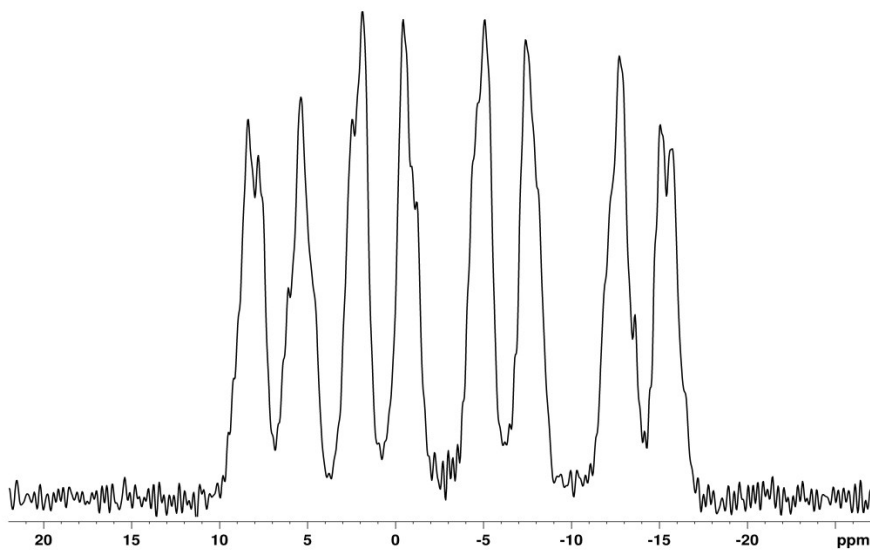


Figure S12. $^{31}\text{P}\{^1\text{H}\}$ CP/MAS solid-state NMR of $[\text{Cu}(\text{PPh}_3)_2(\mu\text{-CH}_3)\text{CuMe}]$ (**2**) accumulated with 16 scans at 162.0 MHz with a MAS spinning speed of 13 kHz.

The quartets are distorted, because the axis of quantization for the quadrupolar copper isotopes is not exactly coincidental with the direction of the applied magnetic field B_0 , due to the Cu quadrupole interaction, which is not small compared to the Cu Zeeman interaction. Under these conditions, MAS is not effective in completely averaging the $^{63,65}\text{Cu}\text{-}^{31}\text{P}$ dipolar interaction. This phenomenon is well known for strong dipolar spin pairs, which also experience a strong

quadrupolar interaction. In the case of compound **2**, the direct ^{63}Cu – ^{31}P dipolar coupling constants are approximately 1.12 kHz (Cu1–P1: 2.258 Å; Cu1–P2: 2.262 Å). As a result, the splittings between adjacent peaks in each quartet are not exactly equal to J . The analysis of such spectra has been described in detail in the literature by Menger and Veeman, and Olivieri.¹³ In case of **2** the analysis is more challenging, because the two phosphorus atoms are not equivalent and probably exhibit a $^2J(^{31}\text{P},^{31}\text{P})$ coupling, and furthermore they are neighbored to two copper atoms, which gives rise to four different isotopomers and probably a $^1J(^{63,65}\text{Cu},^{63,65}\text{Cu})$ coupling, which is unknown. However, the $^{31}\text{P}\{^1\text{H}\}$ CP/MAS solid-state NMR spectrum is in line with the existence of a di-Cu(I), and thus a bridging methyl moiety in the crystal structure of compound **2**.

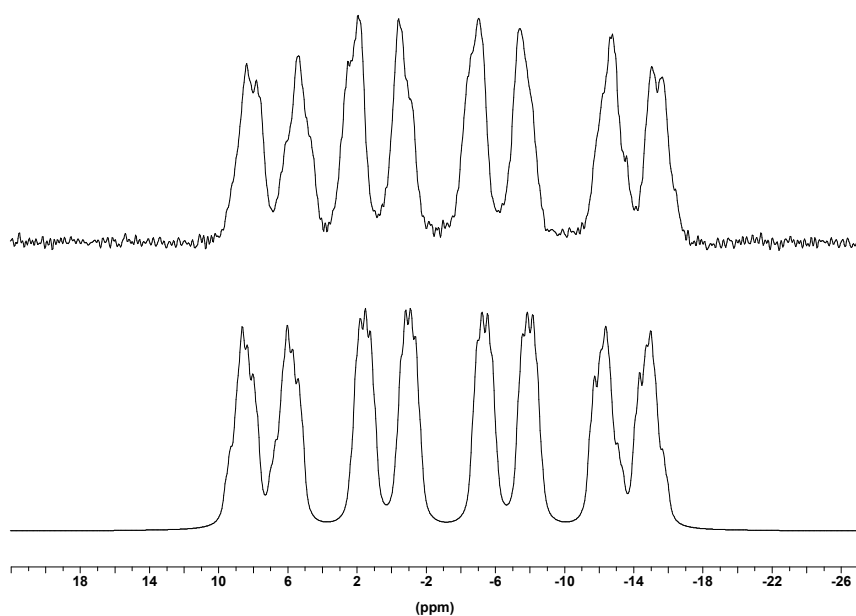


Figure S13. Attempt of a simulation of the $^{31}\text{P}\{^1\text{H}\}$ CP/MAS solid-state NMR of **2** (top) with the spinsystem simulation software WinDaisy using only isotropic J coupling constants (bottom) with the assumed parameters: $\delta^{31}\text{P}_a = -2$, $\delta^{31}\text{P}_b = -4.6$ ppm; ($^1J(^{63}\text{Cu},^{31}\text{P}) = 1100$ Hz, $^2J(^{63}\text{Cu},^{31}\text{P}) = 50$ Hz, $^2J(^{31}\text{P},^{31}\text{P}) = 35$ Hz, $^1J(^{63,65}\text{Cu},^{63,65}\text{Cu}) = 0$ Hz). The ratio for the different isotopomers were calculated to 47.84 : 21.33 : 21.33 : 9.50 %. The coupling constants for $^{1,2}J(^{65}\text{Cu},^{31}\text{P})$ were calculated by multiplication of the coupling constants for $^{1,2}J(^{63}\text{Cu},^{31}\text{P})$ with the factor of the ratio gyromagnetic ratios of 1.071.

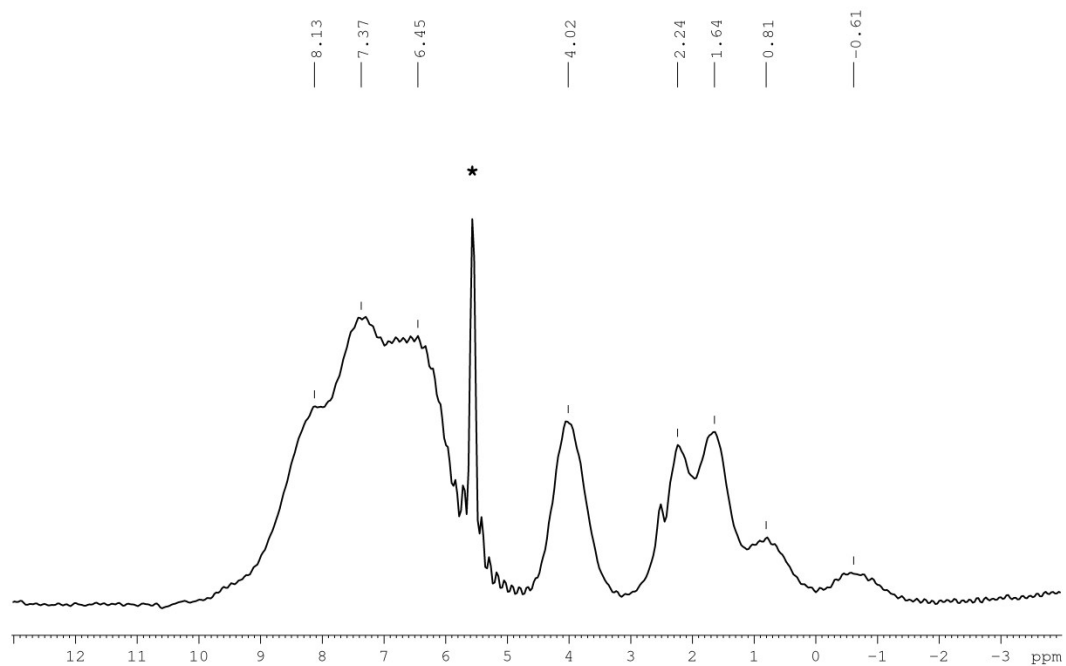


Figure S14. ^1H BR24 Cramps solid-state NMR of **2** measured with 4 scans at 400.15 MHz with a MAS spinning speed of 2 kHz. The spike is marked with an asterisk. The signals at 0.8 and -0.6 ppm were assigned to the CuMe moieties.

NMR Spectra of 2 in D₈-toluene at -40 °C

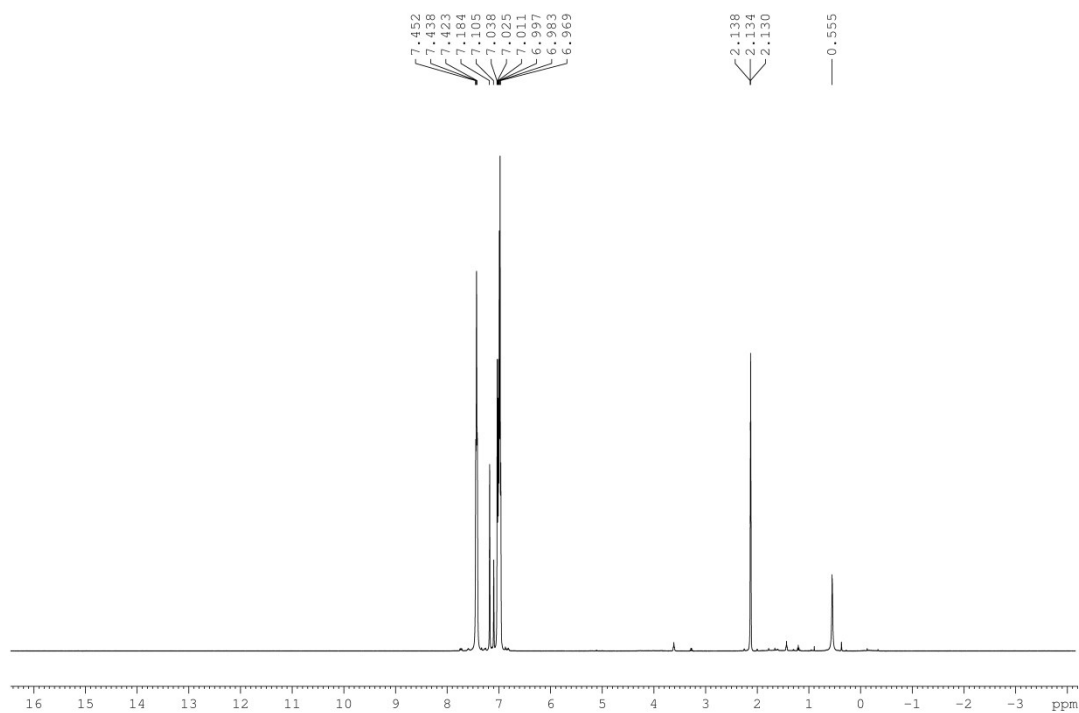


Figure S15. ¹H NMR of **2** in D₈-toluene at -40°C, 500.1 MHz.

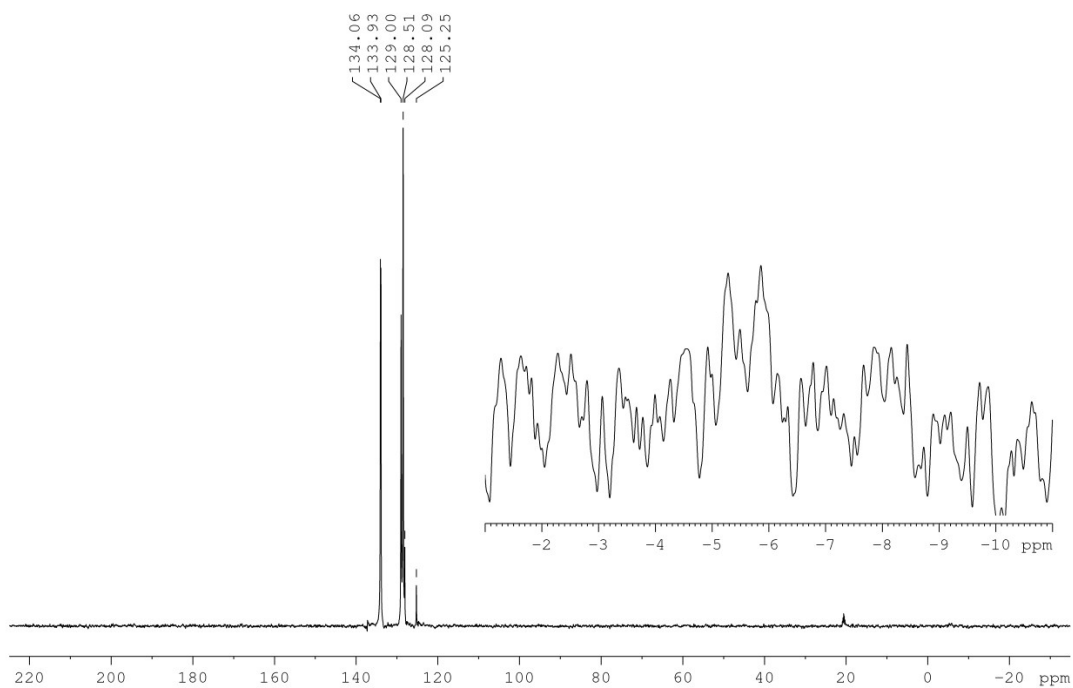


Figure S16. ¹³C{¹H} DEPT135 of **2** in D₈-toluene at -40°C, 125.8 MHz.

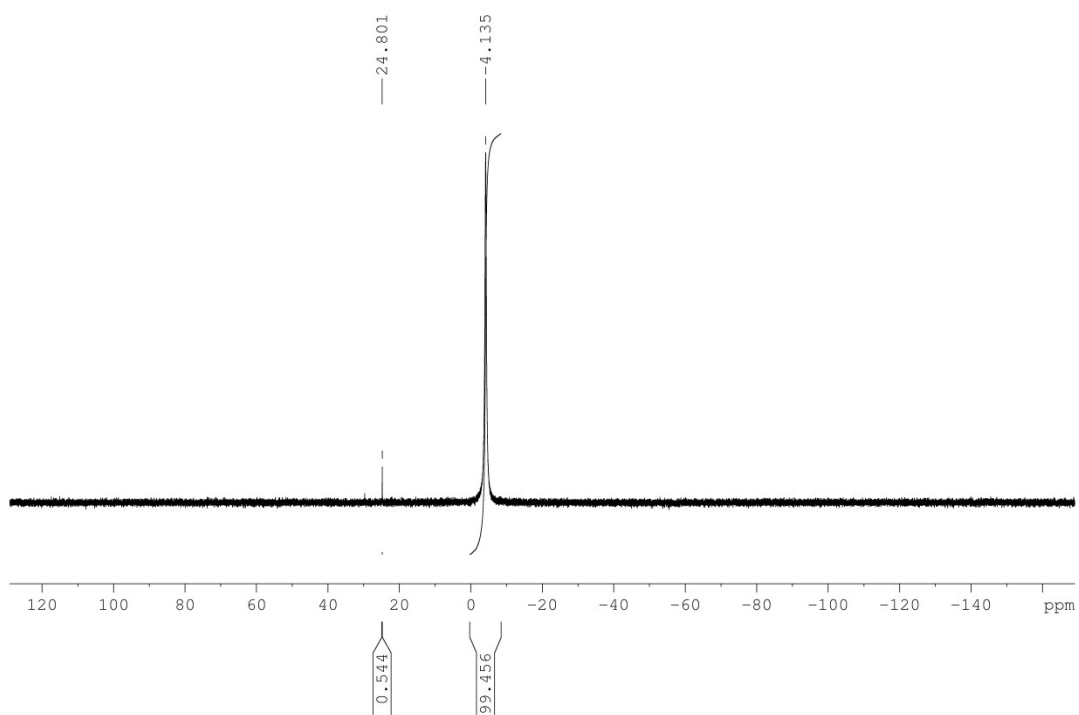


Figure S17. $^{31}\text{P}\{^1\text{H}\}$ NMR of **2** in D_8 -toluene at -40°C , 202.5 MHz.

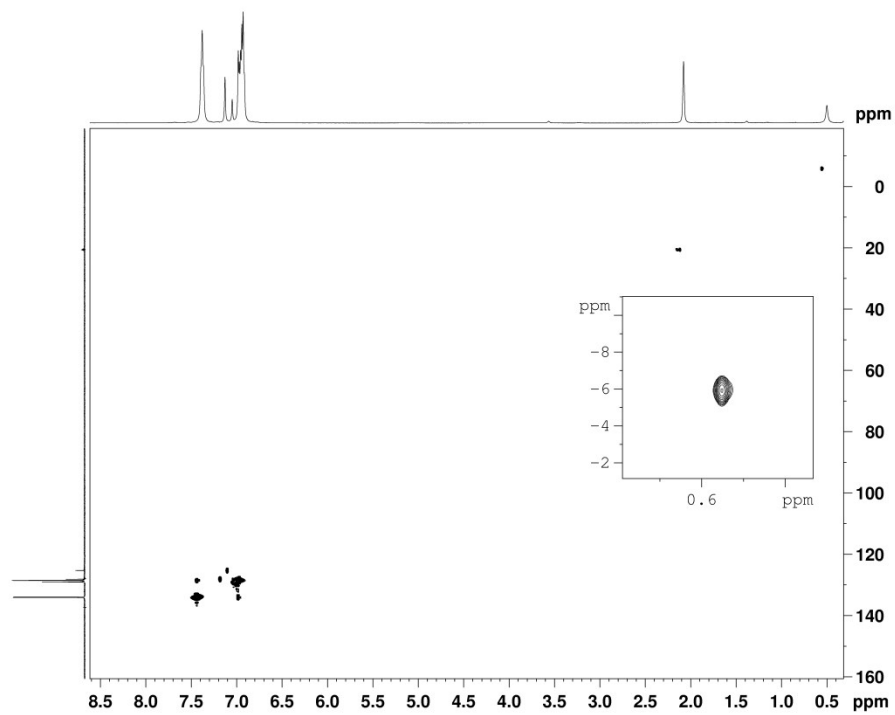


Figure S18. $^{13}\text{C}, ^1\text{H}$ HSQC NMR of **2** in D_8 -toluene at -40°C .

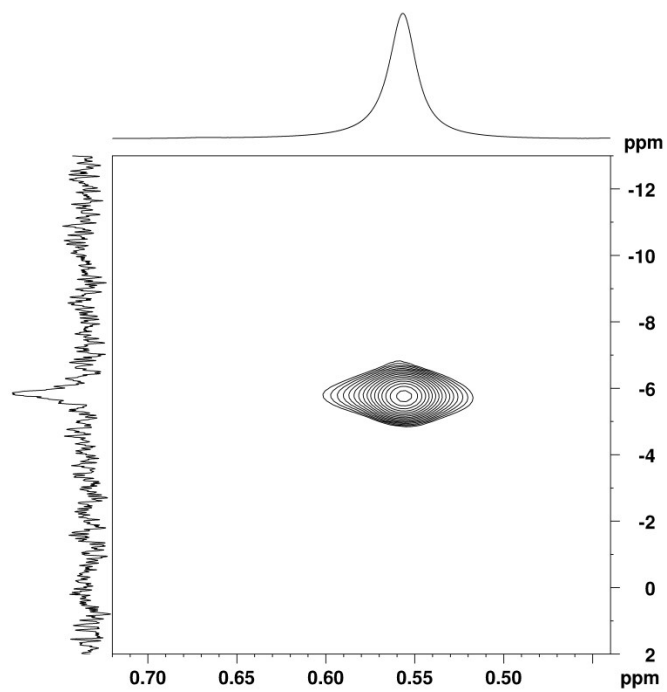


Figure S19. ^1H - ^{13}C HSQC NMR spectrum after dissolving **2** in D_8 -THF, evaporation of the solvent and redissolution in D_8 -toluene at -40°C . The projection in the f1-direction shows the ^{13}C -DEPT135-NMR-spectrum.

NMR Spectra of 2 in d₈-THF at -40 °C

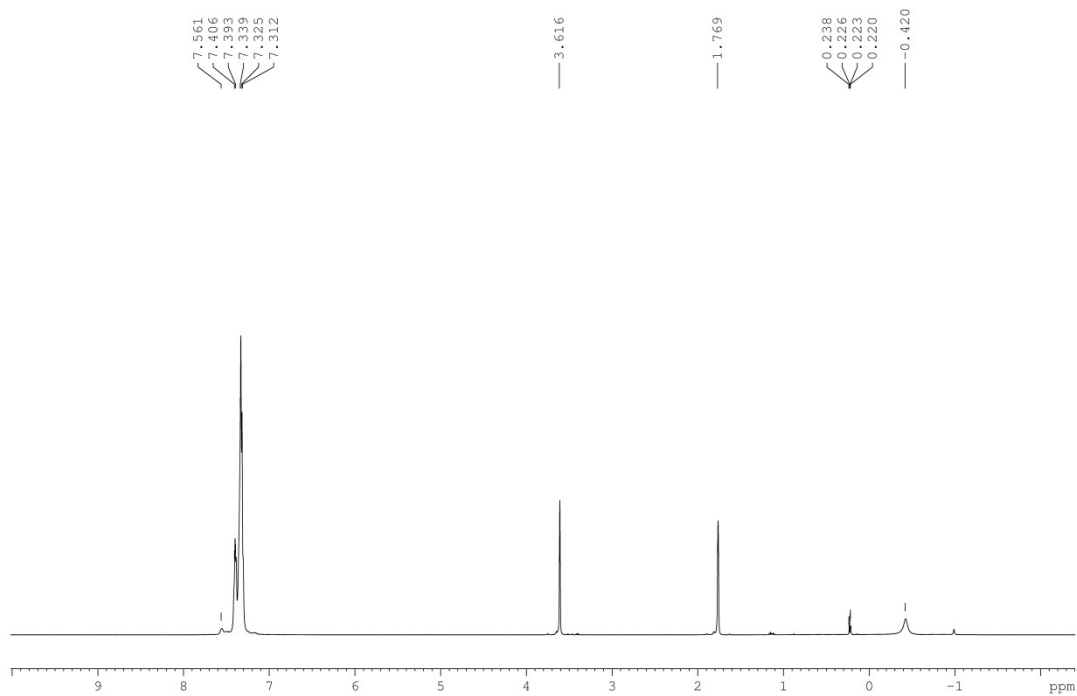


Figure S20. ¹H NMR of 2 in D₈-THF at -40°C, 500.1 MHz.

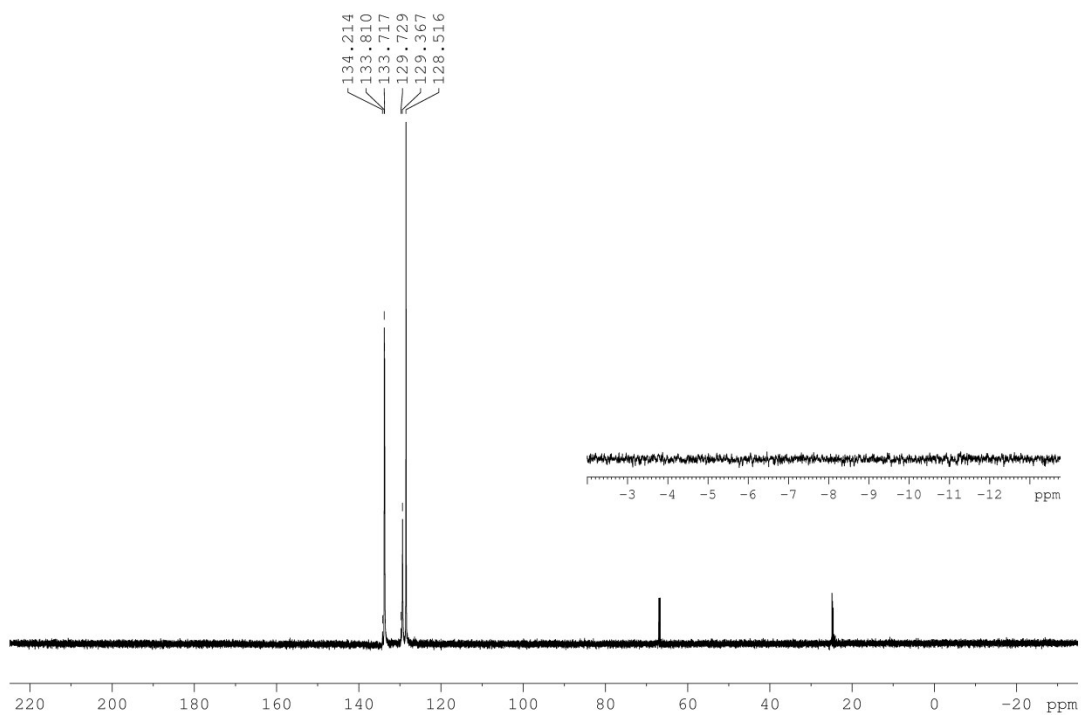


Figure S21. ¹³C{¹H} DEPT135 of 2 in D₈-THF at -40°C, 125.8 MHz.

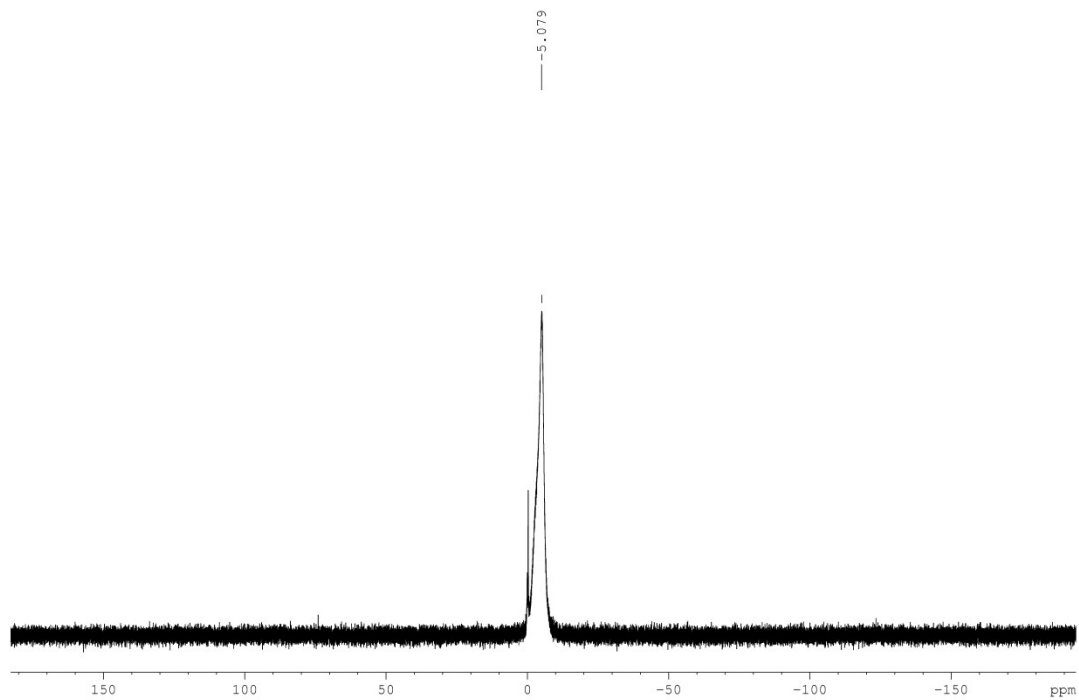


Figure S22. $^{31}\text{P}\{^1\text{H}\}$ NMR of **2** in $\text{D}_8\text{-THF}$ at -40°C , 202.5 MHz.

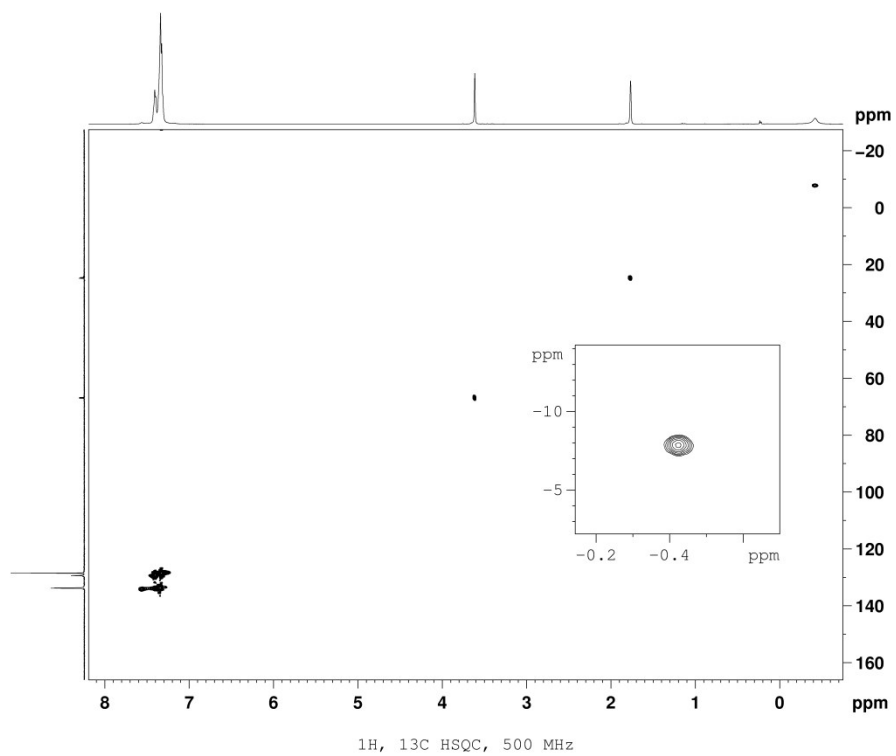


Figure S23. $^{13}\text{C},^1\text{H}$ HSQC NMR of **2** in $\text{D}_8\text{-THF}$ at -40°C .

1. S. Berger and S. Braun, 200 and More NMR Experiments, Wiley-VCH, Weinheim, 2004, p. 141–144.
2. O. V. Dolomanov, L. J. Bourhis, R. J. Gildea, J. A. K. Howard and H. Puschmann, *J. Appl. Crystallogr.*, 2009, **42**, 339-341.
3. F. Neese, *Wires Comput. Mol. Sci.*, 2012, **2**, 73-78.
4. A. D. Becke, *Phys. Rev. A*, 1988, **38**, 3098-3100.
5. J. P. Perdew, *Phys. Rev. B*, 1986, **33**, 8822-8824.
6. F. Weigend and R. Ahlrichs, *Phys. Chem. Chem. Phys.*, 2005, **7**, 3297-3305.
7. A. Schafer, H. Horn and R. Ahlrichs, *J. Chem. Phys.*, 1992, **97**, 2571-2577.
8. D. A. Pantazis, X. Y. Chen, C. R. Landis and F. Neese, *J. Chem. Theory Comput.*, 2008, **4**, 908-919.
9. S. Grimme, S. Ehrlich and L. Goerigk, *J. Comput. Chem.*, 2011, **32**, 1456-1465.
10. S. Grimme, J. Antony, S. Ehrlich and H. Krieg, *J. Chem. Phys.*, 2010, **132**.
11. D. L. Bergman, L. Laaksonen and A. Laaksonen, *J. Mol. Graph. Model.*, 1997, **15**, 301.
12. L. Laaksonen, *J. Mol. Graphics*, 1992, **10**, 33.
13. (a) E. M. Menger and W. S. Veeman, *J. Magn. Reson.*, 1982, **46**, 257-268; (b) J. W. Diesveld, E. M. Menger, H. T. Edzes and W. S. Veeman, *J. Am. Chem. Soc.*, 1980, **102**, 7935-7936; (c) A. Olivieri, *J. Am. Chem. Soc.*, 1992, **114**, 5758-5763; (d) G. Wu and R. E. Wasylshen, *Inorg. Chem.*, 1996, **35**, 3113-3116.